

QCD Glueball Regge Trajectories and the Pomeron

Felipe J. Llanes-Estrada and Stephen R. Cotanch

Department of Physics, North Carolina State University, Raleigh, NC 27695-8202

Pedro J. de A. Bicudo and J. Emilio F. T. Ribeiro

Departamento de Física and Centro de Física das Interações fundamentais, Instituto Superior Técnico, Av. Rovisco Pais, 1049-001 Lisboa, Portugal

Adam Szczepaniak

Department of Physics and Nuclear Theory Center, Indiana University, Bloomington, IN 47405
(October 26, 2018)

Abstract

We report a glueball Regge trajectory emerging from diagonalizing a confining Coulomb gauge Hamiltonian for constituent gluons. Using a BCS vacuum ansatz and gap equation, the dressed gluons acquire a mass, of order 800 MeV , providing the quasiparticle degrees of freedom for a TDA glueball formulation. The TDA eigenstates for two constituent gluons have orbital, L , excitations with a characteristic energy of 400 MeV revealing a clear Regge trajectory for $\vec{J} = \vec{L} + \vec{S}$, where S is the total (sum) gluon spin. Significantly, the $S = 2$ glueball spectrum coincides with the Pomeron given by $\alpha_P(t) = 1.08 + 0.25 t$. Finally, we also ascertain that lattice data supports our result, yielding an average intercept of 1.1 in good agreement with the Pomeron.

Pacs #: 11.55.Jy; 12.39.Mk; 12.39.Pn 12.40.Yx Keywords: Glueball Regge trajectories, Pomeron, QCD, Coulomb gauge Hamiltonian, TDA.

A vintage problem in hadronic physics is to fundamentally explain the observed monotonously rising, to asymptotically flat cross section behavior with increasing Mandelstam variable s . Pre-QCD cross section theorems [1] involving t channel exchanges motivated Pomerenchuk's assertion [2] that vacuum quantum number ($J^{PC} = 0^{++}$) t channel exchanges would describe elastic cross section high energy dependence. Related, it was historically known that hadronic resonances with specific quantum numbers could be connected to a series or "tower" of excited states. From this backdrop the successful Regge picture [3,4], with poles and trajectories linear in t (mass squared), $\alpha(t) = \alpha(0) + b t$, emerged which effectively described cross sections and resonances and therefore unified both scattering and bound state data. Of particular interest in this letter are analyses of high energy diffraction data [5,6] yielding a $J^{PC} = J^{++}$ Regge trajectory with the largest intercept $\alpha(0)$. This trajectory is called the Pomeron and from detailed fits is given by

$$\alpha_P(t) = 1.08 + 0.25 t . \quad (1)$$

Note that by definition, the Pomeron entirely governs and correctly reproduces the high energy scattering behavior since the cross section scales as $s^{\alpha(0)-1}$. The simplicity of this picture is very appealing and the Pomeron remains a contemporary tool for understanding high energy processes, both experimentally and theoretically [7]. In the discussion below we specialize to the soft non-perturbative Pomeron (for an account of the BFKL hard Pomeron in perturbative QCD see [8,9]).

According to Regge theory, the trajectory describing scattering should also be consistent with physical hadron states, implying a $J^{PC} = J^{++}$ trajectory of mesons with slope near 0.25 GeV^{-2} . However, all known hadronic resonances (both mesons and baryons) fall on Chew-Frautschi [10] trajectories with slopes close to 0.9 GeV^{-2} but different intercepts. This is illustrated in Figs. 1 and 2 for several mesons and baryons, respectively, including the ρ whose negative parity, positive G parity tower is well described by $\alpha_\rho(t) = .55 + 0.9 \text{ GeV}^{-2} t$. This incompatibility led to the conjecture that the Pomeron corresponded instead to a Regge trajectory for gluonic states, and most likely one describing the J^{++} glueballs.

Not surprisingly, the gluonic nature of the Pomeron has been widely investigated (see [11] for a recent review) with several recent studies linking the Pomeron and glueball trajectories. From meson trajectories and Wilson loops, Kaidalov and Simonov [12] estimate that the glueball intercept is $\alpha(0) \simeq .7$, while Soloviev [13] computes $\alpha(0) = 1.07 \pm 0.03$ using the quantized elliptic Nambu-Gotto string model. Motivated by the Maldacena conjecture, and solving the dilaton wave equation, Brower, Mathur and Tan [14] obtained a glueball intercept of $\alpha(0) \simeq 1.2$. Finally, using mass relations between the glueball and meson sectors, Brisudova, Burakovsky and Goldman [15] obtain a glueball Regge trajectory with slope $\simeq 0.3 \pm 0.1 \text{ GeV}^2$.

In this communication we report results from a new constituent glueball approach which further strengthens the gluonic Pomeron conjecture. Similar to previous relativistic quark approaches [16,17] yielding a consistent meson Chew-Frautschi Regge slope, our relativistic many-body calculations also produce a glueball Regge trajectory that arises naturally from the confining linear potential and the scale of angular excitations. In reproducing the lattice gauge positive parity glueball spectrum, we obtain a Regge trajectory with intercept near and above unity. Most significantly, the trajectory slope is close to the Pomeron value ($b \approx 0.25 \text{ GeV}^2$) and predominantly independent of model details. Our group has applied

many body techniques to develop a unified approach for the hadron spectrum utilizing a QCD inspired Hamiltonian. Both the gluon [18] and meson [19,20] sectors have been realistically described and a hybrid meson calculation has also recently been completed [21].

We briefly summarize our many-body approach (see refs. [18–20] for complete calculational details). The starting point is a Coulomb gauge, field theoretical Hamiltonian

$$H = Tr \int d\mathbf{x} (\boldsymbol{\Pi}^a \cdot \boldsymbol{\Pi}^a + \mathbf{B}_A^a \cdot \mathbf{B}_A^a) - \frac{1}{2} \int d\mathbf{x} d\mathbf{y} \rho^a(\mathbf{x}) V(|\mathbf{x} - \mathbf{y}|) \rho^a(\mathbf{y}) , \quad (2)$$

with color charge density $\rho^a = f^{abc} \mathbf{A}^b \cdot \boldsymbol{\Pi}^c$ and fields $\boldsymbol{\Pi}^a, \mathbf{B}_A^a = \nabla \times \mathbf{A}^a$. We utilize an instantaneous Cornell potential for confinement, $V = -\frac{\alpha_s}{r} + \sigma r$. The potential parameters are $\alpha_s = .2$, and, from independent lattice results, $\sigma = \frac{3}{4} 0.18 \text{ GeV}^2$. The gluons are then dressed by means of a Bardeen, Cooper and Schrieffer (BCS) ansatz for the vacuum ground state which, through a variational Hamiltonian minimization, generates the gap equation

$$\omega_q^2 = q^2 - \frac{3}{4} \int \frac{d\mathbf{k}}{(2\pi)^3} \hat{V}(|\mathbf{q} - \mathbf{k}|) (1 + (\hat{\mathbf{k}} \cdot \hat{\mathbf{q}})^2) \left(\frac{w_k^2 - w_q^2}{w_k} \right) , \quad (3)$$

for the gluon self-energy, ω_q , containing the dynamical gluon mass. Our potential in momentum space is $\hat{V}(|\mathbf{q} - \mathbf{k}|) = -\frac{4\pi\alpha_s}{(q-k)^2} - \frac{8\pi\sigma}{(q-k)^4}$, where each term generates a divergence in the gap equation (Coulomb is quadratic, confinement is logarithmic). Since we are focusing on confinement we have omitted the Coulomb potential component and then used a cut-off parameter $\Lambda = 4 - 5 \text{ GeV}$ to regularize the remaining logarithmic divergence. Finally, a Tamm-Dancoff (TDA) diagonalization, truncated to the 1p-1h level, is performed for the same field theoretical Hamiltonian (no divergences, Coulomb potential is now included) to generate the glueball spectrum. We used the same linear potential in our quark sector applications which produced reasonable results [19,20], including the appropriate meson Regge slope as indicated by the solid squares in Fig. 1 for the 1^{--} and 3^{--} ρ trajectory. It is important to stress that our quark sector application properly implemented chiral symmetry.

At the more technical level, the glueball TDA state, for fixed orbital, L , and total gluon spin, S , is represented by

$$|\Psi_{LS}^{JPC}\rangle = \sum_{am_1m_2} \int \frac{d\mathbf{q}}{(2\pi)^3} \Phi_{LSm_1m_2}^{JPC}(\mathbf{q}) \alpha_{m_1}^{a\dagger}(\mathbf{q}) \alpha_{m_2}^{a\dagger}(-\mathbf{q}) |\Omega\rangle , \quad (4)$$

where the $\alpha_m^{a\dagger}$ are quasiparticle creation operators acting on the BCS vacuum state $|\Omega\rangle$. The sum is over the color index a and the two transverse spin projections, $m = 1, 2$. The glueball wavefunction has angular momentum composition

$$\Phi_{LSm_1m_2}^{JPC}(\mathbf{q}) = \langle 1m_1 1m_2 | Sm_S \rangle \langle Lm_L Sm_S | Jm_J \rangle \phi_{LS}^{JPC}(q) Y_L^{m_L}(\hat{\mathbf{q}}) . \quad (5)$$

As mentioned above, the gluon quasiparticle energies are obtained from the nonlinear mass gap equation which yields a gluon mass around 800 MeV . Then, with the gap energy, the linear TDA equations are diagonalized for the J^{PC} states of interest, either as a radial equation or variationally in a multi-dimensional Monte Carlo calculation for the Hamiltonian matrix elements using the computer code VEGAS. Our work omits renormalization, but a recently improved, renormalized glueball calculation [22] produced similar $J^{PC} = 0^{\pm+}$

results. Using a new, independent code we have recomputed the glueball spectrum and confirmed our original results [18]. We have also extended the analysis to the maximally acceptable 1p-1h excitation range spanning higher angular momentum states, up to 3^{++} . The 1p-1h energy upper bound is about 3 GeV since it is well known that 2p-2h (4 gluon) states become important for energies twice the lightest 1p-1h excitation ($\approx 1.6 \text{ GeV}$ ground state glueball). A realistic calculation above 3 GeV would entail mixing with 2p-2h states requiring a complicated (4 gluon) Fock space diagonalization. Further, higher angular momentum significantly enhances the interaction spin dependence which is not accurately known. These two reasons are also why we only predict states up to $J = 3$ for the meson spectrum shown in Fig. 1. The positive parity glueball states reliably predicted by our model are compared to the previous and most recent lattice measurements [23] in Fig. 3.

Wavefunction symmetry for two identical bosons requires that $L + S$ must be even. Since the Pomeron should carry positive parity and C-parity, L odd is not considered nor three gluon states which have odd C-parity. Also, according to Yang's theorem, a combination of gluon transversality (Coulomb gauge) and Bose statistics, $J = 1$ states are forbidden for a two gluon system. Further, the $J = 0$ state is precluded from the Pomeron since it necessarily belongs to a lower (daughter) trajectory. Therefore only the $J = 2^{++}$, with $L = 0, S = 2$, and $J = 3^{++}$, with $L = 2, S = 2$, states in Fig. 3 are Pomeron candidates and the corresponding glueball Chew-Frautschi diagram is shown in Fig. 4 along with the Pomeron trajectory.

Figure 4 constitutes the key findings of this study. Notice that our model yields a trajectory with slope $.20 \text{ GeV}^{-2}$ and intercept 1.1, in reasonable agreement with the Pomeron. We found little sensitivity of our results to the confining potential parameter as increasing the strength by 33 % (i.e. $\sigma = \frac{3}{4}0.18 \text{ GeV}^2 \rightarrow 0.18 \text{ GeV}^2$), only marginally reduced the intercept. Further, and of interest to BFKL PQCD studies, our model predicts the soft Pomeron is a correlated two gluon state with total intrinsic spin $S = 2$.

Equally significant are the lattice data which qualitatively supports our main result. The lattice calculations entail some uncertainty and therefore generate a less accurate trajectory having slope $.15 \pm .05 \text{ GeV}^{-2}$. However, the lattice intercept is above unity, although again with appreciable error ($1.1 \pm .5$). We therefore conclude that both our model and recent lattice data are consistent with a glueball interpretation of the Pomeron.

Ideally a $J = 4^{++}$ (and higher) state should also be predicted. This may be possible for lattice calculations but, as discussed above, would be quite formidable in our approach. Conversely, assuming a glueball Pomeron interpretation we can use the fitted trajectory to predict that the 4^{++} and 5^{++} glueballs should have masses $M_J = 2\sqrt{J - 1.08} = 3.42$ and 3.96 GeV , respectively.

Finally, we offer a qualitative explanation for our unified model predictions of meson and Pomeron slope trajectories with respective values $b_{q\bar{q}} \approx 0.9 \text{ GeV}^2$ and $b_{gg} \approx 0.25 \text{ GeV}^2$. In a simple QCD string model with massless partons separated by a string with length r and tension (or energy per unit length) k , the total relativistic mass scales as kr while the angular momentum is proportional to $\frac{1}{2}kr^2$, which generates a Regge trajectory with slope $b = \frac{1}{2\pi kr}$. This string feature is incorporated in our model through the linear confining potential (σr), yielding effective string tensions, $k_{q\bar{q}} = C_{q\bar{q}}\sigma$ and $k_{gg} = C_{gg}\sigma$, for the meson and glueball systems, respectively. Here $C_{q\bar{q}} = \frac{N_c^2 - 1}{2N_c}$ and $C_{q\bar{q}} = N_c$ are the respective quark and gluon color Casimir operators from the density-density Hamiltonian kernel. Hence for

$N_c = 3$ the meson and glueball trajectory slopes are related by $b_{gg} = \frac{C_{q\bar{q}}}{C_{gg}} b_{q\bar{q}} = \frac{4}{9} b_{q\bar{q}}$. While this simple estimate explains much of the meson/glueball slope difference, it is significant that our model is able to account for entirely all of the difference, the rest due to BCS quasiparticle masses and the Coulomb potential in the TDA. It would be very interesting to see if alternative QCD models, particularly the flux tube, can reproduce these results.

In summary, our relativistic many-body approach provides a glueball Regge trajectory similar to the Pomeron diffraction fit. The model also unifies and describes the quark sector by properly implementing chiral symmetry (and breaking) to reproduce the observed meson spectra and attending Regge trajectories with the same, predetermined confining potential. Recent lattice measurements are also consistent with this picture and support a gluonic interpretation of the Pomeron. Reproducing higher J^{++} states on the Pomeron trajectory would confirm this assertion and more sophisticated model calculations are in progress along with a call for alternative model predictions. Finally, our results indicate that the Pomeron provides a worthwhile guiding constraint which future theoretical and experimental glueball studies should utilize.

Pedro Bicudo acknowledges enlightening Pomeron discussions with Barbara Clerbaux, Brian Cox and Mike Pichowsky. This work is supported in part by grants DOE DE-FG02-97ER41048, DE-FG02-87ER40365 and NSF INT-9807009. Felipe J. Llanes-Estrada was a SURA-JLab graduate fellowship recipient and thanks Katja Waidelich for technical help. Supercomputer time from NERSC is also acknowledged.

REFERENCES

- [1] I. Pomeranchuk, Sov. Phys. **3**, 306 (1956); L. Okun and I. Pomeranchuk, Sov. Phys. JETP **3**, 307 (1956); L. Foldy and R. Peirls, Phys. Rev. **130**, 1585 (1963).
- [2] I. Pomeranchuk, Sov. Phys. **7**, 499 (1958).
- [3] T. Regge, Nuovo Cimento **14**, 951 (1959).
- [4] P. D. B. Collins, "Introduction to Regge Theory", (Cambridge University Press, Cambridge, 1977).
- [5] P. V. Landshoff and J. C. Polkinghorne, Nucl. Phys. **B32**, 541 (1971); A. Donnachie and P. V. Landshoff, Nucl. Phys. **B231**, 189 (1984); **B244**, 322 (1984); A. Donnachie and P. V. Landshoff, Phys. Lett. **B185**, 403 (1987); **B437**, 408 (1998).
- [6] M. A. Pichowsky and T.-S. H. Lee, Phys. Lett. **B379**, 1 (1996).
- [7] B. Clerbaux, "Electroproduction Elastique de Mésons ρ à HERA", Ph. D. Thesis (1999); M. A. Pichowsky, "Nonperturbative Quark Dynamics in Diffractive Processes" Ph. D. Thesis (1996).
- [8] E. Kuraev, L. Lipatov, and V. Fadin, Sov. Phys. JETP **45**, 199 (1977); Y. Balitsky and L. Lipatov, Sov. J. Nucl. Phys. **28**, 822 (1978).
- [9] J. Forshaw and D. Ross, "Quantum Chromodynamics and the Pomeron", (Cambridge University Press, Cambridge, 1997).
- [10] G. F. Chew and S. C. Frautschi, Phys. Rev. Lett. **7**, 394 (1961).
- [11] L. Kisslinger and W. Ma, Phys. Lett. **B485**, 367 (2000).
- [12] A. Kaidalov and Y. Simonov, Phys. Lett. **B477**, 163 (2000).
- [13] L. Soloviev, preprint hep-ph/0006010 (2000).
- [14] S. Brower, D. Mathur, and C. Tan, hep-ph/9806344 (1999).
- [15] M. M. Brisudova, L. Burakovsky, and T. Goldman, Phys. Rev. D **58**, 114015 (1998).
- [16] J. Johnson and C. B. Thorn, Phys. Rev. D **13** 1744 (1974); I. Bars and A. J. Hanson, *ibid.* **13**, 1934 (1974).
- [17] F. Iachello, Nimai C. Mukhopadhyay, and L. Zhang, Phys. Rev. D **44**, 898 (1991).
- [18] A. P. Szczepaniak, E. S. Swanson, C.-R. Ji, and S. R. Cotanch, Phys. Rev. Lett. **76**, 2011 (1996).
- [19] F. J. Llanes-Estrada and S. R. Cotanch, Phys. Rev. Lett. **84**, 1102 (2000).
- [20] F. J. Llanes-Estrada and S. R. Cotanch, submitted to Phys. Rev. D.
- [21] F. J. Llanes-Estrada and S. R. Cotanch, Proceedings for Confinement IV, hep-ph/0009191 (2000) and to be published.
- [22] E. Gubankova, C.-R. Ji, and S. R. Cotanch, Phys. Rev. D **62**, 074001 (2000).
- [23] C. J. Morningstar and M. Peardon, Phys. Rev. D **60**, 034509 (1999).
- [24] UKQCD Collaboration, G. S. Bali *et al.*, Phys. Lett. **B309**, 378 (1993).
- [25] H. Chen, J. Sexton, A. Vaccarino, and D. Weingarten, Nucl. Phys. **B34**, 357 (1994).
- [26] M. Teper, hep-th/9812187 (1998).

FIGURES

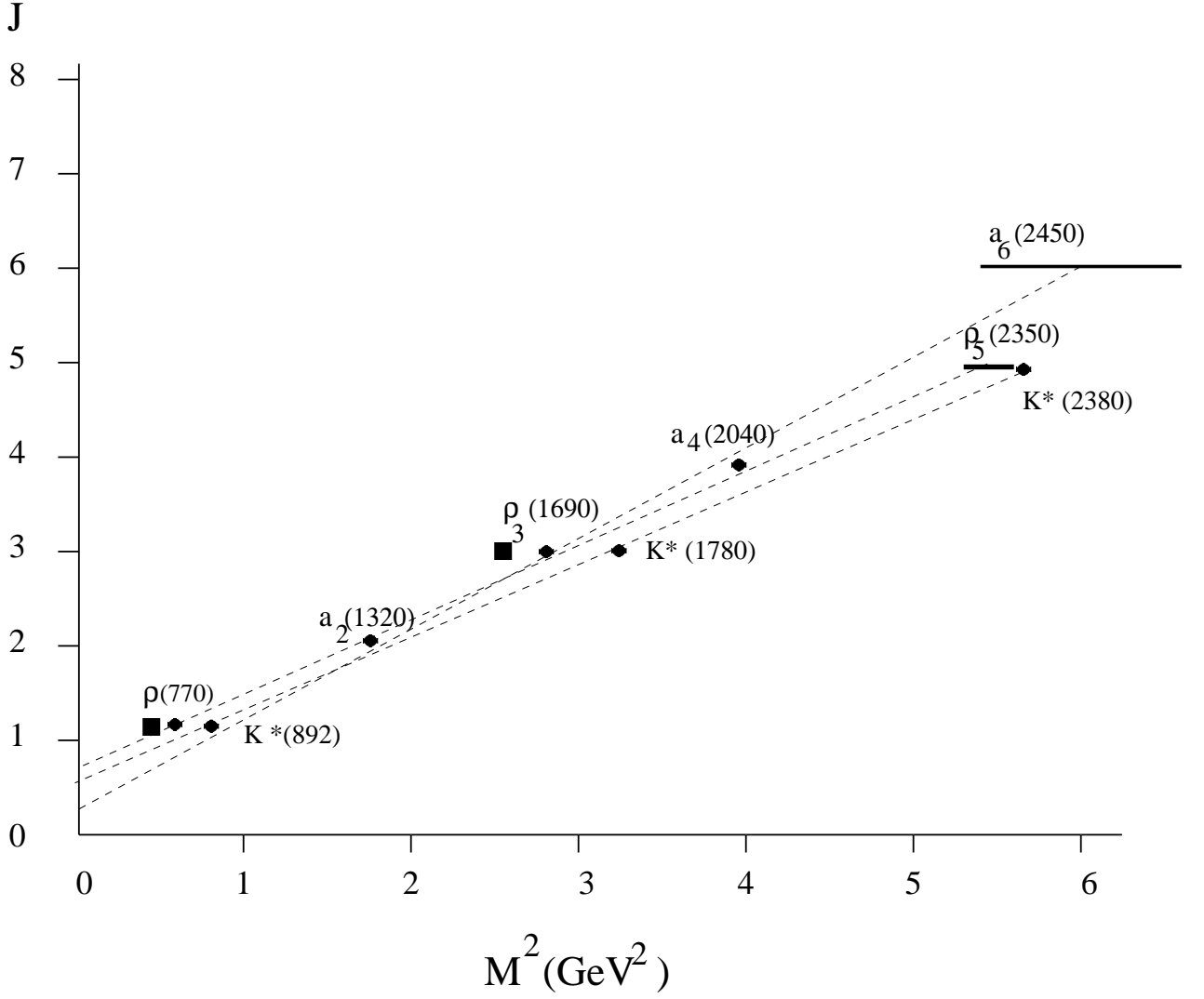


FIG. 1. Meson (ρ , K^* and a) Regge trajectories constructed from recent tabulated data (dark circles and error bars, PDG 2000). Boxes are model TDA predictions for the ρ trajectory.

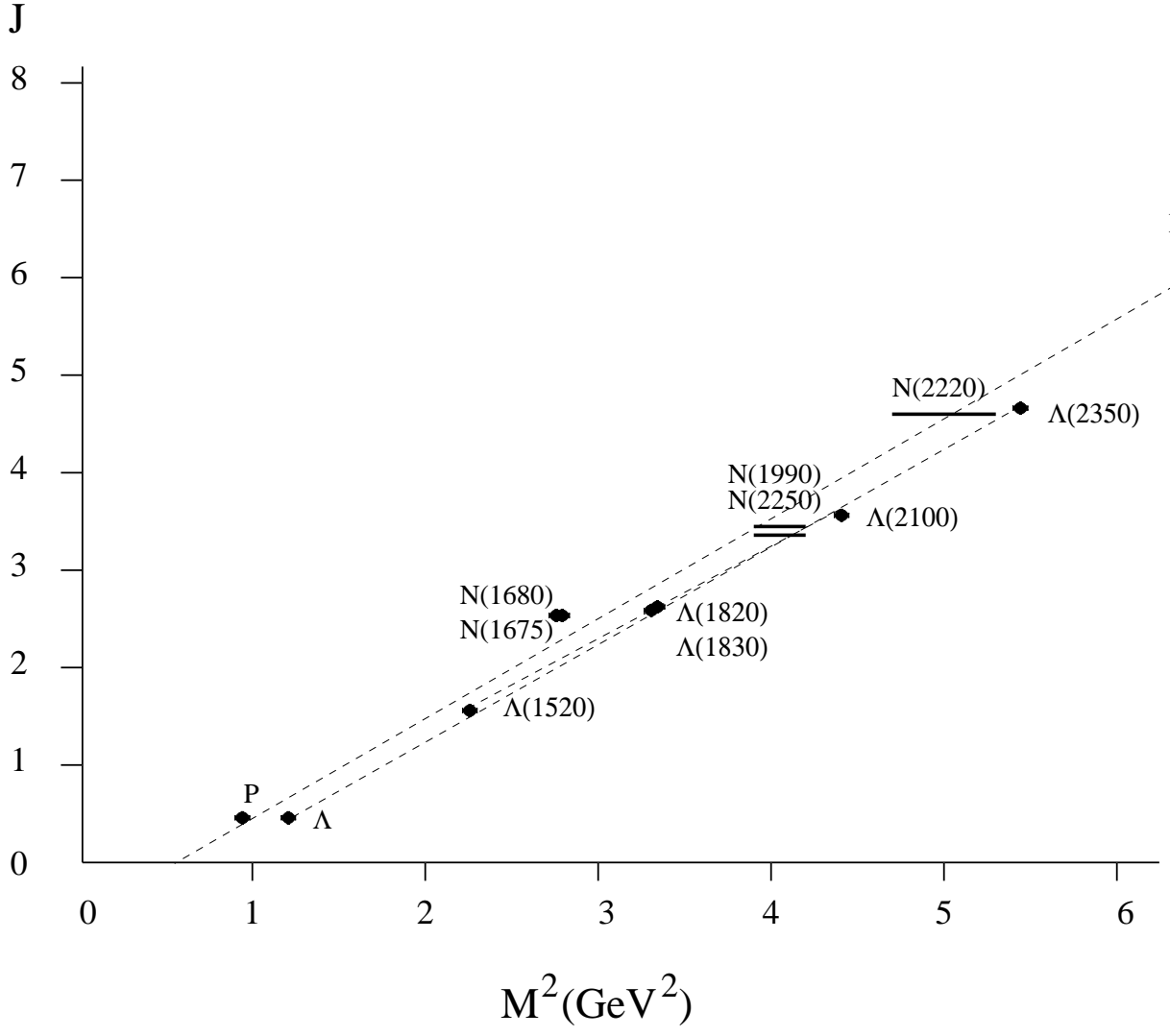


FIG. 2. Baryon (N and Λ) Regge trajectories constructed from recent tabulated data (dark circles and error bars, PDG 2000).

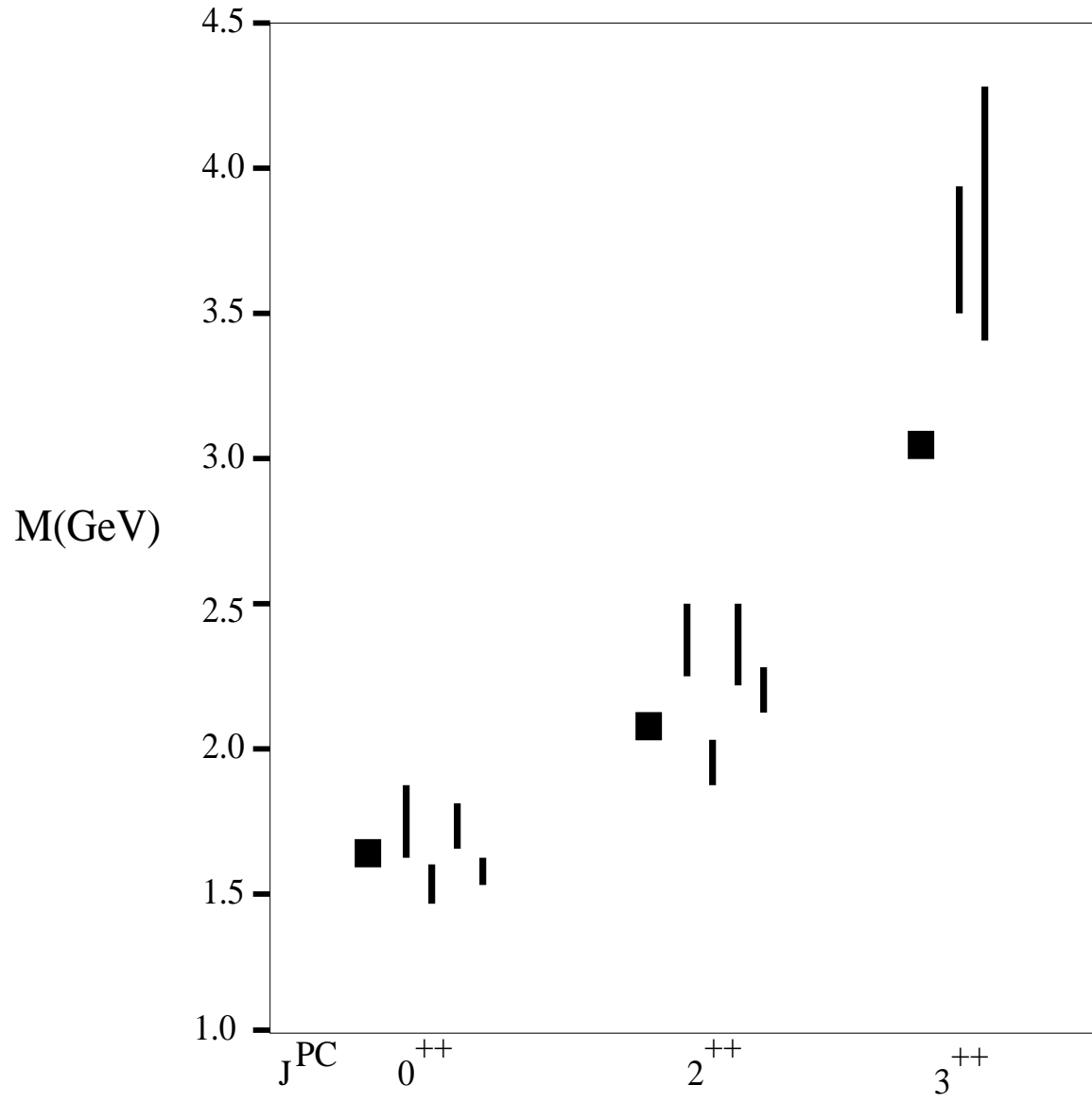


FIG. 3. The TDA (boxes) and lattice gauge (vertical bars showing error) glueball spectra. The lattice results, from left to right, are from refs. [23–26], respectively.

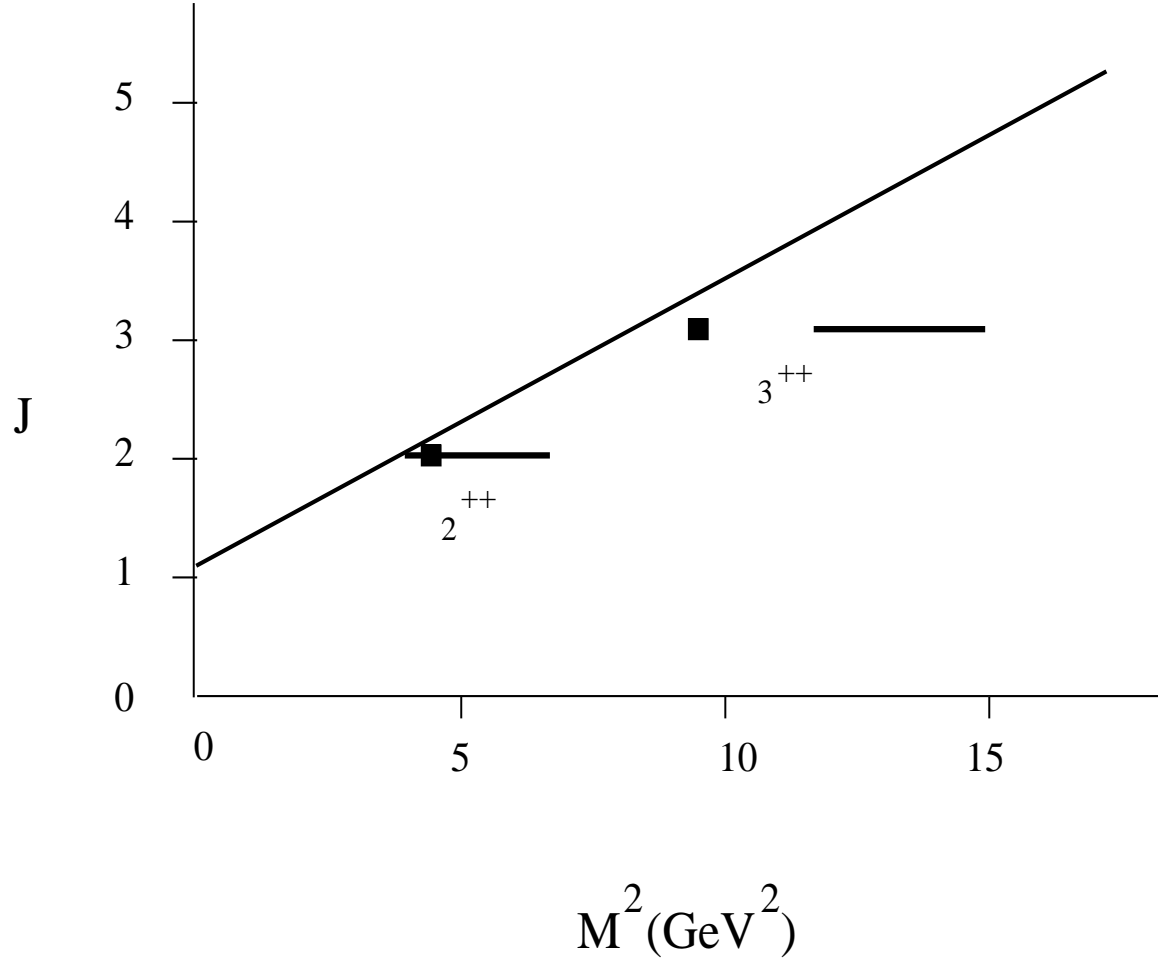


FIG. 4. Comparison of TDA (boxes) and lattice (horizontal bars) J^{++} glueballs with the Pomeron (solid line).